AUV LOCALIZATION IN STRUCTURED UNDERWATER ENVIRONMENTS USING AN *A PRIORI* MAP.

David Ribas [*] **José Neira** [**] **Pere Ridao** [*]
Juan D. Tardós [**]

[*] *Dept. Electrònica, Informàtica i Automàtica. Universitat de Girona. Girona, Spain*
[**] *Dept. Informática e Ingeniería de Sistemas. Universidad de Zaragoza. Zaragoza, Spain*

Abstract: In this paper we describe a localization system for an Autonomous Underwater Vehicle (AUV) which moves in a known and structured underwater environment. A DVL sensor including a compass, two inclinometers and a depth sensor is used to update a simple constant velocity kinematic model. In order to bound the drift inherent of this process, an imaging sonar is used to sense the structures of the environment and to contrast them with the *a priori* map, allowing to refine the robot location in real time. Preliminary experiments in a water tank show the viability of the proposed approach.

Keywords: Robot navigation, Autonomous vehicles, Kalman Filters

1. INTRODUCTION

An essential component of an Autonomous Underwater Vehicle (AUV) for applications in partially known environments is a reliable localization system (Bergem, 1993; Rigaud and Marce, 1991; Carreras *et al.*, 2003). In this paper we describe the localization system of the AUV with which the team of the University of Girona participates in the Student Autonomous Underwater Challenge - Europe (SAUC-E, 2006) event, to be held on England during the summer of 2006.

The goal is to develop an AUV capable of performing various tasks pre-defined by the organization. As usual, the localization of the robot will play an important role in the robot performance. A reliable localization system will be not only useful in the context of the competition, but in many other applications where a map of the environment is available. Inspection of dams, harbors and nuclear reactors are clear examples of applications where a mission is performed within a structured scenario where a map is usually available.

Map-based localization systems have been developed using different types of sensors. Some of the early successful indoor systems used sonar (Leonard and Durrant-Whyte, 1991), laser or infrared range finders (Cox, 1991; Horn and Schmidt, 1995), monocular vision (Lebègue and Aggarwal, 1993; Yagi *et al.*, 1995; Talluri and Aggarwal, 1996), stereo vision (Atiya and Hager, 1993) or even multisensor fusion (Neira *et al.*, 1999). In open outdoor environments, differential GPS can be used to obtain a precise estimation of the vehicle location. However, GPS is unavailable in underwater applications. In these cases, dead-reckoning is an alternative. Unfortunately, dead-reckoning is subject to cumulative errors over time. This may quickly render the vehicle position estimate useless. Most current localization methods make use of range or angle measurements to pre-deployed beacons to bound dead-

reckoning error (Deans and Hebert, 2000; Kantor and Singh, 2002; Olson *et al.*, 2004).

The localization system of our AUV uses a DVL sensor including a compass, two inclinometers and a depth sensor. An extended Kalman filter is used to update a simple constant velocity kinematic model driven by white noise acceleration. The velocity, attitude and depth readings coming from the DVL unit are used to update the pose estimation. In order to bound the drift inherent to this process, an imaging sonar is used to sense planar structures of the environment. Using the pose estimation and an *a priori* map, the location of the surroundings structures (walls) is predicted and compared with the imaging sonar lectures. The discrepancy is used to refine the robot pose, thus avoiding its drift. The details of this algorithm are given in Section 2. Preliminary experiments realized to test the algorithm are described in Section 3. Finally, conclusions are presented in Section 4.

2. LOCALIZATION ALGORITHM

The localization is performed by merging the information of several sensors with an *a priori* map of the environment which is defined as a set of lines $\mathcal{M} = \{\mathbf{l}_{m_1}, \mathbf{l}_{m_2}, \ldots, \mathbf{l}_{m_i}\}$, each one parametrized by ρ_{m_i} and θ_{m_i} (distance and orientation of the walls with respect to the base reference frame). First, an imaging sonar is used to obtain a complete acoustic image of the scene where objects (i.e. the walls of a water tank) can be observed and hence, it is possible to solve for the robot initial position. Then, data from the imaging sonar and the map together with measurements from a DVL are merged within an EKF to obtain a position estimate. In the following subsections the general structure of the localization algorithm are described.

2.1 Initialization

In order to perform localization using an *a priori* map it is necessary to determine the initial position of the vehicle within the mapped environment. Mechanically scanning sonars perform scans in a 2D plane by rotating a sonar beam through a series of small angle steps. For each emitted beam, distance vs. echo-amplitude data is returned forming an acoustic image of the surroundings (Figure 1). The objects (walls) present in the environment appear as high echo-amplitude returns. Hence, it is possible to extract features from which determine the initial position of the vehicle inside the map (Ribas *et al.*, 2006). In the context of the SAUC-E competition, where

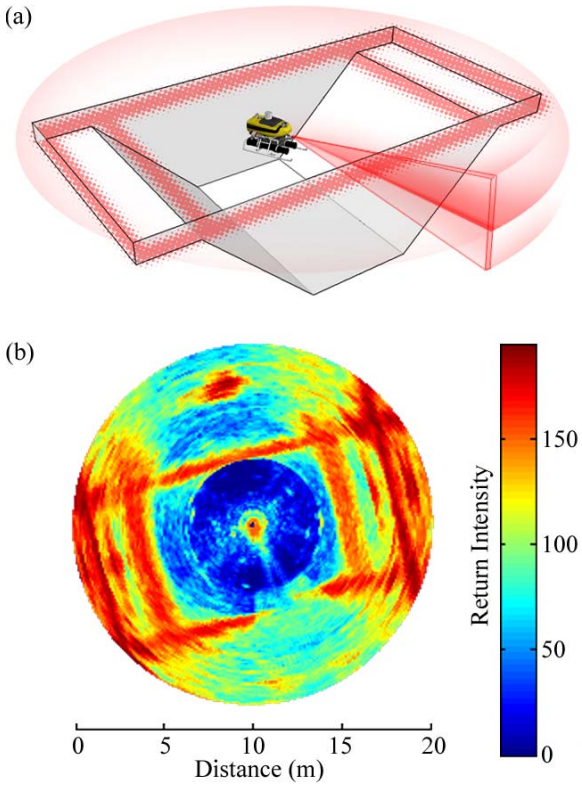

Fig. 1. (a) Schematic representation of the environment where the sonar data were gathered. The highlighted zones represent the expected sonar returns. (b)Image generated from acoustic data

the dimensions and shape of the water tank are well known, a very simple but effective procedure based on the Hough transform (Duda and Hart, 1972) can be used. In our particular case, we don't search for features but directly for the vehicle pose. The Hough voting space is defined as a discretization along the XY coordinates of all the possible vehicle positions inside the water tank playground (Figure 2). Each time a single beam is available, its highest intensity return is selected as the most likely evidence of the presence of the boundary walls (Figure 2b). Each measurement defines a particular zone where the vehicle can exist (Figure 2c). Voting on this zones and accumulating information along a complete 360° scan the position of the vehicle can be determined. As can be seen in Figure 2d, the zone with the highest number of votes is easily identifiable and matches with the actual vehicle position. Assuming that, at the beginning of a mission, the vehicle is stationary (or moving at a low velocity) and that the orientation can be measured with a compass, we can expect a very good position estimate. Hence, choosing a covariance according with the order of magnitude of the Hough space resolution is a good assumption to set the initial position uncertainty.

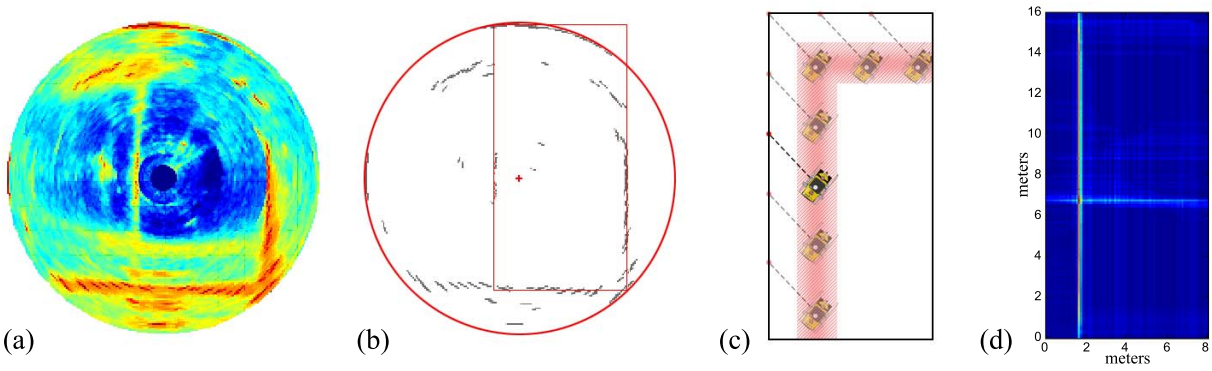

Fig. 2. Initialization of the robot pose. (a) Example of a challenging sonar scan with some spurious data and with the boundaries of the water tank only partially observables. (b) Resulting image after selecting the highest intensity return from each single beam. The boundaries of the water tank are also represented. (c) Diagram of the zone of possible vehicle poses inferred from a single sonar return. (d) Resulting Hough voting space.

2.2 Vehicle pose estimation using a DVL

The above described method needs a complete scan to determine the robot pose. Since mechanically scanned sonars usually need a considerable period of time to obtain a complete scan, this method requires the vehicle to remain stationary while executing the algorithm. For the SAUC-E mission, we need a faster method to solve the navigation, and hence, an improved method using each single beam instead of a bunch of measurements is proposed hereafter.

A SonTek Argonaut DVL unit which includes a compass, 2 inclinometers and a depth sensor is used to estimate the robot pose (navigation problem). Imaging sonar beams are read at 30 Hz while DVL readings arrive asynchronously at a frequency within 1.5 Hz interval. An EKF is used to estimate the 6DOF robot pose whenever a sonar beam is read. DVL readings are used asynchronously to update the filter. To reduce noise inherent to the DVL measurements, a simple 6DOF constant velocity kinematics model is used instead of a more conventional dead reckoning method. Since AUVs are commonly operated describing rectilinear transects at constant speed during survey missions, we believe that the proposed model is a simple but realistic way to describe the motion.

The information of the system at step k is stored in the state vector $\mathbf{x}_k$ with estimated mean $\hat{\mathbf{x}}_k$ and covariance $\mathbf{P}_k$:

$$\hat{\mathbf{x}}_k = [\hat{\eta}^B, \hat{\nu}^R]^T \quad \mathbf{P}_k = E\left[(\mathbf{x}_k - \hat{\mathbf{x}}_k)(\mathbf{x}_k - \hat{\mathbf{x}}_k)^T\right] \quad (1)$$

with:

$$\eta^B = [x, y, z, \phi, \theta, \psi]^T; \quad \nu^R = [u, v, w, p, q, r]^T \quad (2)$$

where, as defined in (Fossen, 1994), η^B is the position and attitude vector referenced to a base frame B, and ν^R is the linear and angular velocity vector referenced to the robot coordinate frame R. The coordinate frame B is oriented to the north. Hence, the compass measurements can be straight forward integrated.

The vehicle movement prediction is performed using a kinematic model such as:

$$\mathbf{x}_k = f(\mathbf{x}_{k-1}) = \begin{bmatrix} \eta_k^B \\ \nu_k^R \end{bmatrix} = \begin{bmatrix} \eta_{k-1}^B + J(\eta_{k-1}^B)\nu_{k-1}^R T \\ \nu_{k-1}^R \end{bmatrix} \quad (3)$$

$$J(\eta) = \begin{bmatrix} c\psi c\theta & c\psi s\theta s\phi - s\psi c\phi & c\psi s\theta c\phi + s\psi s\phi & 0 & 0 & 0 \\ s\psi c\theta & s\psi s\theta s\phi + c\psi c\phi & s\psi s\theta c\phi - s\phi c\psi & 0 & 0 & 0 \\ -s\theta & c\theta s\phi & c\theta c\phi & 0 & 0 & 0 \\ 0 & 0 & 0 & 1 & s\phi t\theta & c\phi t\theta \\ 0 & 0 & 0 & 0 & c\phi & -s\phi \\ 0 & 0 & 0 & 0 & s\phi/c\theta & c\phi/c\theta \end{bmatrix} \quad (4)$$

Although in this model the velocity is considered to be constant, in order to allow for slight movements, the velocity perturbation is modelled as the integral of a stationary white noise v_k with a diagonal $\mathbf{Q}$ in the order of magnitude of the maximum acceleration increment that the robot can experiment over a sample period.

$$\nu_k^R = \hat{\nu}_k^R + v_k T \quad (5)$$

$$E[v_k] = 0; \quad E[v_k, v_j^T] = \delta_{k_j} \mathbf{Q} \quad (6)$$

Hence, the acceleration noise is additive in the velocity (Equation 5) and propagates nonlinearly to the position. Finally, the model prediction and update is carried out as detailed below:

2.2.1. Prediction The estimate of the state is obtained as:

$$\hat{\mathbf{x}}_k = f(\hat{\mathbf{x}}_{k-1}) \quad (7)$$

and its covariance matrix as:

$$\mathbf{P}_k = \mathbf{F}_k \mathbf{P}_{k-1} \mathbf{F}_k^T + \mathbf{G}_k \mathbf{Q}_k \mathbf{G}_k^T \quad (8)$$

where $\mathbf{F}_k$ and $\mathbf{G}_k$ are the Jacobian matrices of partial derivatives of the non-linear model function f with respect to the state $\mathbf{x}^B_{R,k}$ and the noise v_k, respectively.

2.2.2. Update using DVL measurements The model prediction is updated by the standard Kalman filter equations each time a new DVL measurement arrives:

$$\mathbf{z}_{S,k} = [u_b, v_b, w_b, u_w, v_w, w_w, \phi_i, \theta_i, \psi_c, z_{depth}]^T \quad (9)$$

Where subindex b stands for bottom tracking velocity, w for through water velocity, i for inclinometers and c represents the compass. The measurement model is:

$$\mathbf{z}_{S,k} = \mathbf{H}_{S,k}\mathbf{x}_{k|k-1} + w_k \quad (10)$$

$$\mathbf{H}_S = \begin{bmatrix} \mathbf{0}_{3\times3} & \mathbf{0}_{3\times3} & \mathbf{I}_{3\times3} & \mathbf{0}_{3\times3} \\ \mathbf{0}_{3\times3} & \mathbf{0}_{3\times3} & \mathbf{I}_{3\times3} & \mathbf{0}_{3\times3} \\ \mathbf{0}_{3\times3} & \mathbf{I}_{3\times3} & \mathbf{0}_{3\times3} & \mathbf{0}_{3\times3} \\ 0\ 0\ 1 & \mathbf{0}_{1\times3} & \mathbf{0}_{1\times3} & \mathbf{0}_{1\times3} \end{bmatrix} \quad (11)$$

where w_k (measurement noise) is a zero-mean white noise:

$$E[w_k] = 0; \quad E[w_k, w_j^T] = \delta_{k_j}\mathbf{R}_{S,k} \quad (12)$$

Since the DVL sensor provides a status measurement for the bottom tracking and water velocity, depending on the quality of the measurements, different versions of the H matrix are used to fuse one (removing row 2), the other (removing row 1), or both readings (using the full matrix).

2.3 Correction with the a priori map and an imaging sonar

Herein, the information obtained from the imaging sonar together with the *a priori* map $\mathcal{M}$ is used to perform a correction of the vehicle state estimate. Whenever a new single beam (not a complete acoustic image) is obtained from the imaging sonar, the highest return is chosen. This measurement is the most likely to pertain to any object present in the scene and as a consequence, to a feature in the *a priori* map. We will use this information to perform an update of the EKF presented above and correct the state estimate. The high intensity return $\mathbf{z}_{P,k}$ is a point represented in polar coordinates with respect to the vehicle frame R:

$$\mathbf{z}_{P,k} = [\rho_p, \theta_p]^T; \quad \hat{\mathbf{z}}_{P,k} = \mathbf{z}_{P,k} + u_k \quad (13)$$

Where $\mathbf{z}_{P,k}$ would be the value obtained if noise u_k was not present. The noise u_k is a zero-mean white Gaussian noise:

$$E[u_k] = 0; \quad E[u_k, u_j^T] = \delta_{k_j}\mathbf{R}_{P,k} \quad (14)$$

We need to determine the the correspondence between the measurement and the objects in the map. First, the cartesian coordinates of the measurement $\mathbf{z}_{P,k}$ need to be obtained:

$$\begin{bmatrix} x_p \\ y_p \end{bmatrix} = q(\mathbf{z}_{P,k}) = \begin{bmatrix} \rho_p cos\ \theta_p \\ \rho_p sin\ \theta_p \end{bmatrix} \quad (15)$$

$$\mathbf{S}_k = \mathbf{J}_q\mathbf{R}_{P,k}\mathbf{J}_q^T \qquad where \qquad \mathbf{J}_q = \frac{\partial q}{\partial \mathbf{z}_{P,k}} \quad (16)$$

$\mathbf{S}_k$ represents the uncertainty of the point in cartesian coordinates and $\mathbf{J}_q$ is the Jacobian matrix of the q function with respect to the measurement $\mathbf{z}_{P,k}$. The next step is to define each line $\mathbf{l}_{m_i} = [\rho_{m_i}, \theta_{(m_i)}]^T$ from the map $\mathcal{M}$ by its orientation and its distance to the origin with respect to the vehicle coordinate frame R:

$$\begin{bmatrix} \rho^R_{m_i} \\ \theta^R_{m_i} \end{bmatrix} = g(\mathbf{l}_{m_i}, \mathbf{x}) = \begin{bmatrix} \rho_{m_i} - x^B cos\ \theta_{m_i} - y^B sin\ \theta_{m_i} \\ \theta_i - \psi^B \end{bmatrix} \quad (17)$$

$$\mathbf{J}_g = \frac{\partial g}{\partial \mathbf{x}_k} \quad (18)$$

$\mathbf{J}_g$ is the Jacobian of the g function. As the map is assumed perfectly known, the uncertainty only depends on the vehicle state $\mathbf{x}$. With both the sonar return and the map in the same reference frame, an implicit measurement equation stating that the point belongs to the line can be defined (Castellanos and Tardós, 1999):

$$h(g(\mathbf{x}), q(\mathbf{z})) = \rho^R_{m_i} - x_p cos\ \theta^R_{m_i} - y_p sin\ \theta^R_{m_i} = 0 \quad (19)$$

$$\mathbf{H}_1 = \frac{\partial h}{\partial(\rho^R_{m_i}, \theta^R_{m_i})} \cdot \mathbf{J}_g; \quad \mathbf{H}_2 = \frac{\partial h}{\partial(x_p, y_p)} \cdot \mathbf{J}_q \quad (20)$$

Where $\mathbf{H}_1$ and $\mathbf{H}_2$ are the Jacobians of the implicit measurement function h with respect to the sonar return and a line of the map. To produce the update, an association hypothesis between the measurement and one of the lines from the map is needed. For this purpose, an individual compatibility test is performed using the presented measurement equation:

$$D^2 = h^T(\mathbf{H}_1\mathbf{P}_{k|k-1}\mathbf{H}_1^T + \mathbf{H}_2\mathbf{R}_{P,k}\mathbf{H}_2^T)^{-1}h < \chi^2_{d,\alpha} \quad (21)$$

Distance D^2 is the Mahalanobis distance. The correspondence is accepted if the distance is less than $\chi^2_{d,\alpha}$, with α defined as the confidence level and $d = dim(h)$. The Nearest Neighbor (NN) selection criterion determines that among the features that satisfy (21), the one with the smallest Mahalanobis distance is chosen and the association hypothesis is accepted. This association process ensures not only the correct association of the measurement but also allows rejecting spurious data from the sonar image, such those produced by multipath.

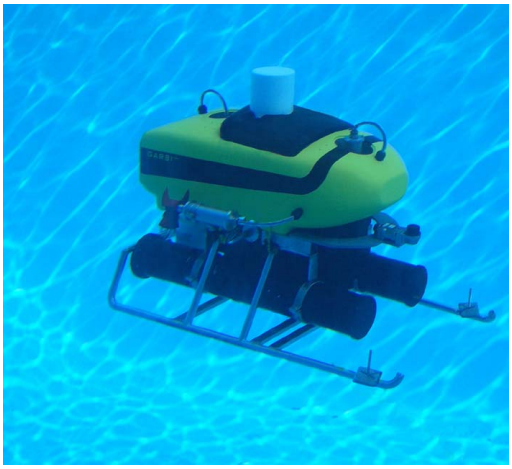

Fig. 3. The GARBI^{AUV}

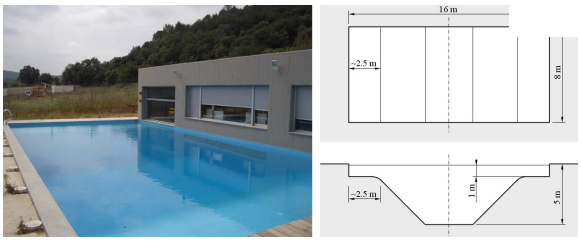

Fig. 4. Water tank at the Research Center on Underwater Robotics of the University of Girona

Having the data association solved, an update of the vehicle state estimate can be performed using the EKF equations for an implicit measurement function:

$$\mathbf{K}_k = \mathbf{P}_{k|k-1}\mathbf{H}_1^T(\mathbf{H}_1\mathbf{P}_{k|k-1}\mathbf{H}_1^T + \mathbf{H}_2\mathbf{R}_{P,k}\mathbf{H}_2^T)^{-1} \quad (22)$$

$$\hat{\mathbf{x}}_k = \hat{\mathbf{x}}_{k|k-1} - \mathbf{K}_k h(\hat{\mathbf{x}}_k, \hat{\mathbf{z}}_k) \quad (23)$$

$$\mathbf{P}_k = (\mathbf{I} - \mathbf{K}_k\mathbf{H}_1)\mathbf{P}_{k|k-1} \quad (24)$$

3. EXPERIMENTAL RESULTS

We carried out an experiment with the GARBI^{AUV} (See Figure 3) in the water tank of the Underwater Robotics Research Center at the University of Girona (See Figure 4). The vehicle was equipped with a Miniking Imaging sonar from Tritech, a sensor designed for use in underwater applications like obstacle avoidance and target tracking. It can perform scans in a 2D plane by rotating a fan-shaped sonar beam of 3° of horizontal beamwidth and 40° of vertical beamwidth. During the experiment, the sensor was set up to work within a range of 10 meters, capturing a sonar return every 0.1 meters (100 measurements per beam). Its scanning rate was set to the maximum (around 6 seconds per a 360° scan).

In order to estimate the vehicle movement an Argonaut DVL from Sontek was used. The DVL is

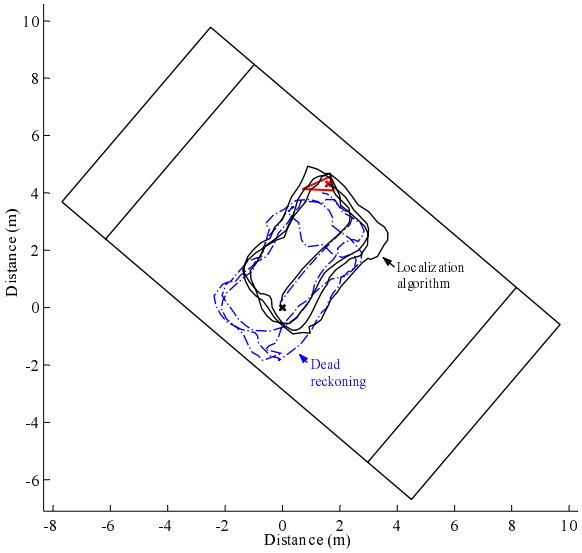

Fig. 5. Trajectory from the localization algorithm vs. dead reckoning trajectory represented within the *a priori* map.

a sensor specially designed for ROV/AUV applications which measures ocean currents and vehicle speed over ground, by means of the Doppler shift effect, and altimetry. Moreover, the unit is also equipped with a compass/tilt sensor which permits to recollect attitude data, a pressure sensor to estimate the depth and a temperature sensor for sound speed calculations.

The GARBI^{AUV} carried out a guided trajectory of around 42 meters, consisting on several loops; 161 complete sonar scans were taken. Although no ground truth information is available, the vehicle was commanded taking as a reference the water tank boundaries in order to ensure the overlapping of the different loops.

The results are shown in Figure 5. For comparison purposes the trajectory estimated using dead reckoning of the DVL measurements (blue dash-dotted line) is represented together with the one estimated using the imaging sonar and the localization algorithm (black line). It is also represented the map used to perform the localization. As it can be seen, the dead reckoning trajectory has an important drift, which is controlled using the proposed localization algorithm.

4. CONCLUSION

The main contribution of the presented work is to perform localization in a structured environment using a DVL and an imaging sonar to navigate through an *a priori* map. In this document, a post-processed experimental test has been carried out in order to show the potential of the proposed technique. However, in the final application the algorithm should run in real time over the control

architecture of the SAUC-E vehicle. As long as the computational cost is not great and that the problem dimension is bounded, it is expected to fulfill the real-time requirements.

ACKNOWLEDGMENT

This research has been funded in part by the Dirección General de Investigación of Spain under projects DPI2003-07986 and DPI2005-09001-C03-01. Authors also want to acknowledge the sponsors who made possible our participation in the SAUC-E competition (see the team homepage at *http://eia.udg.es/sauce*).

REFERENCES

Atiya, S. and G.D. Hager (1993). Real-time vision-based robot localization. *IEEE Trans. Robotics and Automation* **9**(6), 785–800.

Bergem, O. (1993). A multibeam sonar based positioning system for an AUV. In: *Eighth International Symposium on Unmanned Untethered Submersible Technology (AUSI)*.

Carreras, M., P. Ridao, R. Garcia and T. Nicosevici (2003). Vision-based localization of an underwater robot in a structured environment. In: *IEEE International Conference on Robotics and Automation ICRA'03*. Taipei, Taiwan.

Castellanos, J.A. and J.D. Tardós (1999). *Mobile Robot Localization and Map Building: A Multisensor Fusion Approach*. Kluwer Academic Publishers, Boston.

Cox, I.J. (1991). Blanche - an experiment in guidance and navigation of an autonomous robot vehicle. *IEEE Transactions on Robotics and Automation* **7**, 193–204.

Deans, M. and M. Hebert (2000). Experimental comparison of techniques for localization and mapping using a bearings only sensor. In: *Proc. of the ISER 00 Seventh International Symposium on Experimental*. Springer- Verlag. pp. 395–404.

Duda, R.O. and P.E. Hart (1972). Use of the Hough transformation to detect lines and curves in pictures. *Communications of the ACM*.

Fossen, T.I. (1994). *Guidance and Control of Ocean Vehicles*. John Wiley & Sons Ltd.

Horn, J. and G. Schmidt (1995). Continuous localization of a mobile robot based on 3d-laser-range-data, predicted sensor images and dead-reckoning. *Journal of Robotics and Autonomous Systems, Special Issue "Research on Autonomous Mobile Robots"* **14**, 99–118.

Kantor, G.A. and S. Singh (2002). Preliminary results in range-only localization and mapping. In: *Proceedings of the IEEE Conference on Robotics and Automation*. pp. 1818–1823.

Lebègue, X. and J.K. Aggarwal (1993). Significant line segments for an indoor mobile robot. *IEEE Trans. Robotics and Automation* **9**(6), 801–815.

Leonard, J.J. and H.F. Durrant-Whyte (1991). Mobile robot localization by tracking geometric beacons. *IEEE Transactions on Robotics and Automation* **7**(3), 376–382.

Neira, J., J. Horn, J.D. Tardós and G. Schmidt (1999). Fusing range and intensity images for mobile robot localization. *IEEE Transactions on Robotics and Automation* **15**(1), 76–84.

Olson, E., J. Leonard and S. Teller (2004). Robust range-only beacon localization. In: *Proceedings of Autonomous Underwater Vehicles*. pp. 66–75.

Ribas, D., J. Neira, P. Ridao and J.D. Tardós (2006). SLAM using an imaging sonar for partially. In: *Proceedings of IEEE/RSJ International Conference on Intelligent Robots and Systems*.

Rigaud, V. and L. Marce (1991). Absolute location of underwater robotic vehicles by acoustic data fusion. In: *Autonomous Mobile Robots: Perception, Mapping, and Navigation (Vol. 1)* (S. S. Iyengar and A. Elfes, Eds.). pp. 185–190. IEEE Computer Society Press. Los Alamitos, CA.

SAUC-E (2006). *http://www.dstl.gov.uk/news_events/competitions/sauce/index.php*.

Talluri, R. and J.K. Aggarwal (1996). Mobile robot self-location using model-image feature correspondence. *IEEE Trans. Robotics and Automation* **12**(1), 63–77.

Yagi, Y., Y. Nishizawa and M. Yachida (1995). Map-based navigation for a mobile robot with omnidirectional image sensor COPIS. *IEEE Trans. Robotics and Automation* **11**(5), 634–648.